Eur Biophys J (2012) 41:875–890
DOI 10.1007/s00249-012-0817-5

REVIEW

EBSA
Biophysics in Europe

Model-based approaches for the determination of lipid bilayer structure from small-angle neutron and X-ray scattering data

Frederick A. Heberle · Jianjun Pan · Robert F. Standaert · Paul Drazba · Norbert Kučerka · John Katsaras

Received: 16 February 2012 / Revised: 29 March 2012 / Accepted: 15 April 2012 / Published online: 16 May 2012

Abstract Some of our recent work has resulted in the detailed structures of fully hydrated, fluid phase phosphatidylcholine (PC) and phosphatidylglycerol (PG) bilayers. These structures were obtained from the joint refinement of small-angle neutron and X-ray data using the scattering density profile (SDP) models developed by Kučerka et al. (Biophys J 95:2356–2367, 2008; J Phys Chem B 116:232–239, 2012). In this review, we first discuss models for the standalone analysis of neutron or X-ray scattering data from bilayers, and assess the strengths and weaknesses inherent to these models. In particular, it is recognized that standalone data do not contain enough information to fully resolve the structure of naturally disordered fluid bilayers, and therefore may not provide a robust determination of bilayer structure parameters, including the much-sought-after area per lipid. We then discuss the development of matter density-based models (including the SDP model) that allow for the joint refinement of different contrast neutron and X-ray data, as well as the implementation of local volume conservation within the unit cell (i.e., ideal packing). Such models provide natural definitions of bilayer thicknesses (most importantly the hydrophobic and Luzzati thicknesses) in terms of Gibbs dividing surfaces, and thus allow for the robust determination of lipid areas through equivalent slab relationships between bilayer thickness and lipid volume. In the final section of this review, we discuss some of the significant findings/features pertaining to structures of PC and PG bilayers as determined from SDP model analyses.

Keywords Lipid bilayer · Bilayer structure · Area per lipid · Bilayer thickness · Molecular dynamics simulations · Fluid phase

Special Issue: Scattering techniques in biology—Marking the contributions to the field from Peter Laggner on the occasion of his 68th birthday.

F. A. Heberle (✉) · J. Pan · J. Katsaras
Biology and Soft Matter Division, Neutron Sciences Directorate, Oak Ridge National Laboratory, Oak Ridge, TN 37831-6100, USA
e-mail: heberlefa@ornl.gov

R. F. Standaert
Biosciences Division, Energy and Environmental Sciences Directorate, Oak Ridge National Laboratory, Oak Ridge, TN 37831-6100, USA

R. F. Standaert
Department of Biochemistry and Molecular and Cellular Biology, The University of Tennessee, Knoxville, TN 37996, USA

P. Drazba · J. Katsaras
Department of Physics and Astronomy, The University of Tennessee, Knoxville, TN 37996-1200, USA

N. Kučerka · J. Katsaras
Canadian Neutron Beam Centre, National Research Council, Chalk River, ON K0J 1J0, Canada

N. Kučerka
Department of Physical Chemistry of Drugs, Faculty of Pharmacy, Comenius University, 832 32 Bratislava, Slovakia

J. Katsaras
Joint Institute for Neutron Sciences, Oak Ridge National Laboratory, Oak Ridge, TN 37831-6453, USA

Introduction

Some of the great scientific achievements of the twentieth century have resulted from the field of structural and molecular biology. For example, much effort has gone into elucidating the form, and hence function, of the genome and proteome. Yet it is much more recently that the lipidome has begun to receive its due consideration. One reason for this lag is the technical challenge of accurately determining lipid structure and dynamics. Nucleic acids and proteins are characterized at the level of individual molecules, where form is understood in terms of precise positions of individual atoms within a molecule, and function is understood in terms of their motions. In contrast, the active form and function of lipids are often collective phenomena that emerge at the level of supramolecular ensembles (i.e., mesoscopic scale). These ensembles are intrinsically disordered and hence unsuitable for study by atomic-resolution techniques, such as X-ray and neutron crystallography, which have transformed structural biology.

The landmark fluid mosaic model proposed by Singer and Nicolson (1972) describes the overall organization and function of biological membranes. These authors, well aware of the diverse nature of membranes, sought generalizations that were applicable to all of them. With the widespread acceptance of the fluid mosaic model, the focus has turned progressively toward the membrane's finer details. As methods for isolating relatively pure membrane fractions improved, a wide variation in lipid composition between the various cellular membranes (e.g., plasma membrane, mitochondrial inner and outer membranes, endoplasmic reticulum, Golgi, etc.) was revealed (van Meer and de Kroon 2011). One then questions why such lipid diversity exists, or indeed, is necessary. The answer, simply put, is that lipid composition plays a vital role in membrane structure and function (Spector and Yorek 1985).

In this regard, it has become clear that membrane lipids (collectively, the lipidome) do more than form a passive envelope that acts as a permeability barrier between the outer and inner regions of a cell, or a passive matrix in which membrane proteins function. Rather, lipids actively participate in critical cellular functions and have a rich metabolism of their own. As is the case with other biomolecules, lipid production varies with time, and is subject to myriad chemical transformations by enzymatic and non-enzymatic processes. One biological arena where lipids are known to play a prominent role is signaling, and this field of study has emerged as an important discipline within the biological and medical sciences. In signaling pathways, lipids are typically transformed by enzymatic hydrolysis, phosphorylation, dephosphorylation or oxidation into new molecules, which serve as diffusible secondary messengers that interact with downstream receptors (Hannun and Obeid 2008; Wymann and Schneiter 2008).

Biological membranes typically contain several hundred lipid species, which possess unique properties that are ideally suited to their various functions. The hydrophobic nature of their tails makes for an excellent barrier that is impermeable, or selectively permeable, to molecules that readily dissolve in water. The diversity in hydrocarbon tail structure provides adaptability to multiple environments, and leads to distinct phases such as liquid-disordered and gel, and with the addition of sterols, liquid-ordered phases. Non-ideal interactions between different lipid species (for example, those with saturated and unsaturated chains) can drive the formation of compositionally distinct domains, which are thought to play important roles in diverse cellular phenomena, including protein sorting and transmembrane signaling (Lingwood and Simons 2010). Membrane fluidity is an important property that is homeostatically regulated by the incorporation of sterols, as well as variation in fatty acyl chain length, degree of unsaturation and double-bond geometry. For example, by changing membrane composition, cells are able to adapt to altered nutrient supply and environmental changes (e.g., temperature, chemicals and pressure). This adaptability is central to the ability of bacteria (Zhang and Rock 2008) and poikilothermic organisms (Hazel 1995) to survive.

With few exceptions, biological membranes exist in a disordered, fully hydrated state, a fact that presents unique challenges to elucidating their fine structure. Despite the many techniques that have been applied to study these complex systems, robust, quantitative structural information has remained elusive (Nagle and Tristram-Nagle 2000b). Traditional crystallographic methods and high-resolution NMR techniques are generally ill-equipped to address the problem. In this review, we discuss how specialized neutron and X-ray scattering methods can nonetheless be applied to the study of membrane systems, particularly in conjunction with simulation. Specialized NMR methods also provide highly useful, generally complementary information, and the reader is referred to a recent review by Leftin and Brown (2011).

For membrane systems, the real-space information content of a scattering experiment is the scattering length density (SLD) profile. However, individual atomic positions are not well localized in the thermally disordered bilayer, and are best described by broad statistical averages. The fluid bilayer structure is therefore a low-resolution picture of the distributions of groups of neighboring atoms whose SLDs contrast with those of adjacent groups.

Several methods exist for determining bilayer structure from diffraction data. Fourier reconstruction of neutron or X-ray structure factors directly yields the bilayer's SLD

profile, from which the locations of structural features can be inferred. For example, X-ray scattering clearly resolves lipid headgroups because of the large electron density contrast between the electron-rich phosphate groups and the surrounding hydrocarbon and aqueous regions, which have a much lower electron density. Depending on whether light water (H_2O) or heavy water (D_2O) is used to hydrate the bilayers, neutron scattering is sensitive to carbonyl (C=O) groups. Both carbon and oxygen have positive scattering lengths, whereas hydrogen (^1H) has a negative scattering length, so the scattering length density changes relatively sharply at the boundary between the hydrocarbon and carbonyl regions of the bilayer. As a result, neutron SLD (NSLD) profiles establish the bilayer's hydrocarbon and overall thickness with great precision.

Neutron diffraction can, however, be taken one step further, owing to the large scattering length difference between hydrogen and deuterium. When a deuterium atom is introduced at a specific site in a lipid, the difference between NSLD profiles of the protiated and deuterated bilayers reveals the position of the deuteron. In principle, site-specific deuteration therefore allows for the detailed determination of bilayer structure using the different NSLD profiles. In a classic series of papers, Büldt et al. used this technique to establish the structure of gel and fluid phase dipalmitoylphosphatidylcholine (DPPC) bilayers (Büldt et al. 1978, 1979; Zaccai et al. 1979). However, the enormous amount of work required to solve even a single bilayer structure (including the synthesis of multiple deuterated variants of the lipid, and data collection for all of the protiated and deuterated samples) renders this method impractical as a general tool.

In addition to the direct Fourier synthesis of structure factors, inverse Fourier methods have also been widely used to elucidate bilayer structure. In this model-based technique, the distributions of sub-molecular scattering components are represented with simple functional forms from which form factors can be easily calculated (via Fourier transform) and compared to experimentally determined form factors through a refinement procedure. Models have several advantages over direct Fourier reconstruction. Specifically, they do not suffer from Fourier truncation effects, and more importantly, they allow for the simultaneous analysis of different types of data (including both neutron and X-ray scattering data). The model-based approach developed in the last 20 years has proven very fruitful, particularly for establishing the structure of fully hydrated, fluid phase bilayers. In the first part of this review, we discuss real-space models for bilayer structure, culminating in the SDP model developed by Kučerka et al. (2008, 2012). We then discuss some of the significant SDP findings pertaining to the structures of phosphatidylcholine (PC) and phosphatidylglycerol (PG) bilayers.

Models of bilayer structure

Sample considerations

The primary data used in modeling bilayer structure is the continuous form factor $F(q)$ (shown schematically in Fig. 1), which is obtained from the observed neutron or X-ray scattered intensity $I(q)$ from a bilayer. The sample can consist either of multilamellar bilayer stacks (in an aqueous vesicle suspension or oriented on a flat substrate) or individual bilayers (unilamellar vesicles in aqueous suspension). Before beginning our discussion of bilayer structural models, we will briefly discuss the properties of these samples in the context of a scattering experiment.

Multilamellar samples

Multilamellar samples can be fabricated to either be aligned (i.e., bilayer normals are all pointing in the same direction) or not aligned (i.e., bilayer normals are isotropically distributed), with the latter samples frequently referred to as powder samples. The simplest type of bilayer preparation is the powder multilamellar vesicle (MLV) suspension, which is prepared by hydrating a dry lipid film with an aqueous buffer, followed by mechanical dispersion (Bangham et al. 1965). MLVs consist of many tens of bilayers arranged in concentric spheres, separated by layers of water (Hope et al. 1986). Oriented bilayer stacks are prepared by depositing a solution of lipid (dissolved in a suitable organic solvent) onto a flat substrate (typically a glass coverslip or a single crystal of silicon), and allowing the solvent to evaporate

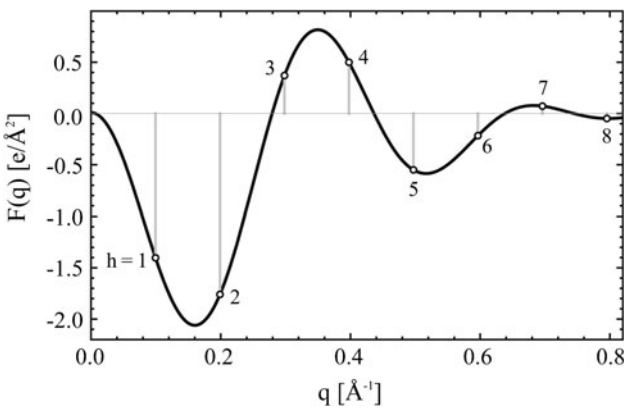

Fig. 1 Schematic representation of a bilayer's continuous X-ray form factor $F(q)$. $F(q)$ is related to the experimentally observed scattered intensity $I(q)$ as $|F(q)| = \sqrt{I(q)P(q)}$, where $P(q)$ includes corrections for sample geometry and vesicle polydispersity. The form factor for a centrosymmetric structure is always real [i.e., $+F(q)$ or $-F(q)$]. The phase information that is lost in the experiment is the sign of $F(q)$. Diffraction from multilamellar samples results in a discrete sampling of $F(q)$ at integer multiples (diffraction orders h) of $q = 2\pi/d$, where d is the lamellar repeat distance

(Levine and Wilkins 1971; Tristram-Nagle 2007), leaving behind a film consisting of stacks of aligned bilayers. The amount of lipid is adjusted relative to the area of the substrate, such that the stack is generally composed of a few thousand bilayers. Hydration is achieved from the vapor phase, and the degree of hydration is controlled by adjusting the relative humidity in the sample chamber through the use of saturated salt solutions (Obrien 1948; Young 1967). Compared to the ease of preparing a fully hydrated MLV suspension, it is considerably more difficult to achieve full hydration from the vapor phase (Katsaras 1997, 1998), and specially designed sample chambers are required (Katsaras and Watson 2000).

For many bilayer-forming lipids, the balance of attractive and repulsive forces between the polar interfaces of neighboring bilayers results in a water layer of well-defined thickness separating individual bilayers in the stack (Rand and Parsegian 1989). A perfect lattice of bilayers superimposes a structure factor of delta functions on I(q), concentrating the scattered intensity into discrete Bragg peaks. As shown in Fig. 1, these peaks effectively "sample" I(q) at integer multiples of $q = 2\pi/d$, where the lamellar repeat distance d is the sum of the lipid bilayer and water layer thicknesses. In an aligned sample, scattering arising from the in-plane and out-of-plane bilayer structure is spatially segregated along the axes of a two-dimensional detector (Katsaras et al. 1995, 2000; Raghunathan and Katsaras 1995). The random orientation of unaligned samples causes a powder averaging of both in-plane and out-of-plane structural information, distributing the scattering intensity into concentric rings with respect to the incident beam, with a concomitant reduction in signal-to-noise ratio if a two-dimensional detector is not used to accept all of the scattered intensity.

Under favorable sample conditions of low lattice disorder, up to four Bragg orders can generally be observed from MLV samples (Pabst et al. 2000), and 8–10 Bragg orders from oriented samples (Katsaras and Stinson 1990; Hristova and White 1998). For fluid phase bilayers, samples must often be partially dehydrated in order to achieve this result, with the caveat that dehydration may change the bilayer structure in nonlinear ways (Nagle and Tristram-Nagle 2000b; Tristram-Nagle and Nagle 2004). Determining the structure of a fully hydrated, fluid phase MLV sample presents additional challenges. For example, at full hydration, increased bilayer undulation typically results in lattice disorder (disorder of the second kind, characterized by a non-uniform unit cell), effectively redistributing the Bragg intensity into the peak's tails (Zhang et al. 1994). The resulting diffuse scattering can be accounted for with a modified structure factor using Caillé theory (Zhang et al. 1994; Lemmich et al. 1996; Pabst et al. 2000), and continuous form factors up to 0.5 Å^{-1} have been obtained with this approach (Pabst et al. 2000). Lyatskaya et al. (2001) and Liu and Nagle (2004) developed a diffuse scattering analysis for oriented bilayers, allowing for the determination of the continuous form factor up to 0.8 Å^{-1}. In principle, diffuse scattering provides additional physical insight (e.g., bilayer bending and compression moduli), though analysis is less straightforward than the standard method of integrating Bragg peak intensities.

Unilamellar samples

MLV sample preparations are converted into a suspension of unilamellar single-bilayer vesicles (ULVs) by extrusion through polycarbonate filters of defined pore size. These vesicles have a mean diameter that is similar to the filter's pore size, and typically exhibit some polydispersity, which must be accounted for in the data analysis (Kiselev et al. 2002; Pencer et al. 2006). Small ULVs (SUVs) prepared by sonication (Huang 1969) range in size between 100 and 300 Å (Tenchov et al. 1985), and have been used in scattering experiments (Wilkins et al. 1971) (SUVs are however not commonly used to obtain detailed structural information, as it is thought that their high degree of curvature may affect lipid packing). At dilute ULV concentrations (<2 weight percent), enough water is present between vesicles to eliminate the particle-particle structure factor, thus simplifying the determination of the continuous bilayer form factor (Kučerka et al. 2007b). However, the necessity of working at dilute concentrations can reduce the signal-to-noise of a ULV sample relative to an MLV sample, therefore limiting the information that can be realistically obtained. Despite this limitation, fully resolved structures can be obtained using only ULV data. This is done by including in the analysis several different contrast scattering data sets, in addition to lipid volume data obtained from independent measurements (discussed in detail below).

Neutron and X-ray scattering data contain different information

Neutrons and X-rays scatter differently from the same chemical groups making up a bilayer, resulting in complementary structural information. For a protiated lipid in 100 % H_2O, these differences are most apparent in the headgroup region, as shown in Fig. 2. X-rays scatter strongly from the electron-rich phosphate group (highlighted in the inset to Fig. 2b), allowing for the robust determination of the phosphate–phosphate distance between adjacent leaflets in the bilayer (Nagle and Tristram-Nagle 2000b). On the other hand, because of hydrogen's negative neutron scattering length, neutron scattering experiments are strongly sensitive to differences in hydrogen content in adjacent regions of the bilayer. The lipid ester-carbonyl groups (highlighted in the

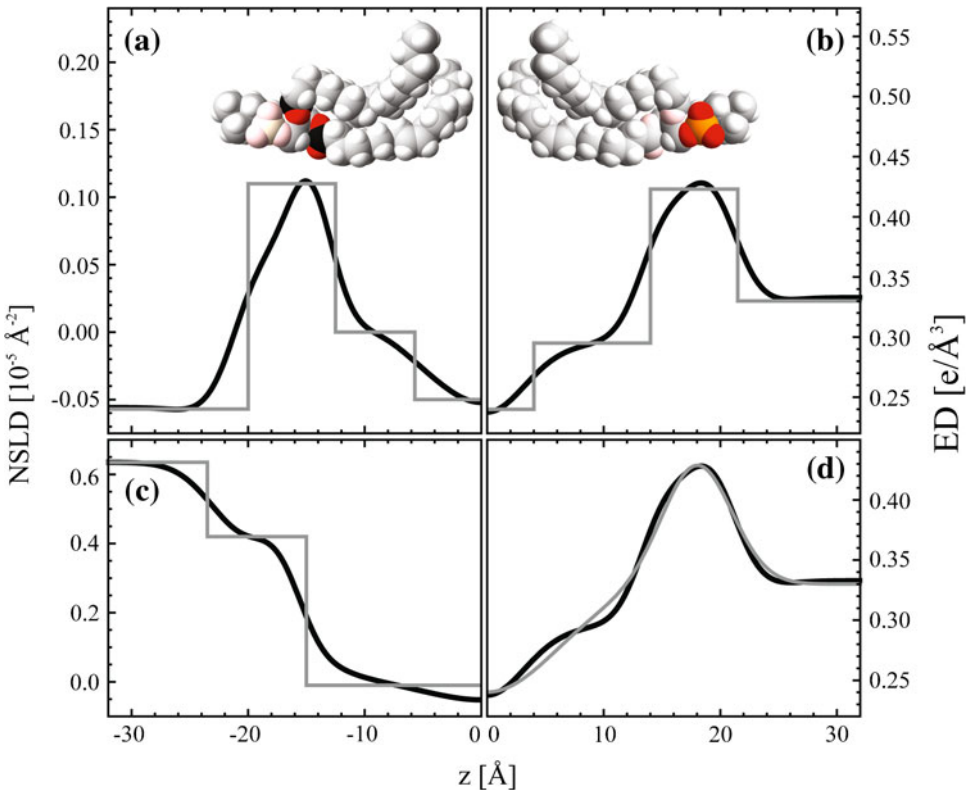

Fig. 2 Schematic representation of a bilayer's neutron scattering length density (NSLD) and electron density (ED) profiles with strip and Gaussian models. An NSLD (**a**) and ED profile (**b**) for protiated lipid in H_2O (*black*) described by a hypothetical 4-strip model (*gray*). Starting from the bilayer center at $z = 0$, the strips correspond roughly to the methyl trough, methylene plateau, headgroup and water layer. *Insets* to these panels show a space-filling model of DOPC with its ester-carbonyl (**a**) and phosphate (**b**) groups *highlighted*, demonstrating the general position of these groups with respect to the peak position of the NSLD and ED profiles. (**c**) A 3-strip model for the NSLD of protiated lipid in 100 % D_2O, with strips corresponding roughly to the hydrocarbon region, headgroup and water layer. (**d**) A two-Gaussian model for the ED profile

inset to Fig. 2a), which contain no hydrogen, show up much better in an NSLD profile than either the methylenes, making up the hydrocarbon chains, or the PC headgroup (Wiener and White 1992b). Furthermore, because water solvates the headgroup and penetrates down to the glycerol/carbonyl region, the NSLD contrast between the headgroup and acyl chains can be modified simply by changing the D_2O/H_2O ratio in which the sample is prepared (compare Fig. 2a–c). The ability to generate independent data sets using different contrast versions of the same system (including deuterated variants of the lipid) in order to highlight different bilayer components is a distinct advantage of neutron scattering experiments.

A one-dimensional real-space model of bilayer structure describes the time-averaged distribution of scattering length density or matter, projected onto the bilayer normal. For mathematical tractability, models are invariably the sum of simple functional forms representing the distinct chemical moieties of the bilayer. These regions are often simplified as strips of constant value, or Gaussians, and are specified by two or three parameters, respectively. A particular bilayer structure corresponds to a set of fixed parameter values from which the continuous bilayer form factor is evaluated via a Fourier transform and compared to the experimentally determined form factor (either discrete or continuous values). The most probable structure thus corresponds to the parameter set that minimizes the differences (e.g., in a least-squares sense) between the predicted and observed form factors.

There are two basic approaches to modeling the real-space bilayer structure. For standalone neutron or X-ray scattering data, it is often desirable to directly model the scattering length density. However, a more general approach is to model the matter distribution of submolecular components, from which either neutron or X-ray SLD profiles are obtained when multiplied by the appropriate scattering lengths.

Models for standalone (neutron or X-ray) data

Strip models

Strip or slab models are the simplest models used to describe bilayers, whereby the neutron or X-ray SLD is

approximated by strips of constant density. Each strip is described by two fitting parameters (e.g., a height and a width), and the number of strips used is a compromise between fidelity to the underlying SLD (which favors more strips) and the requirement that the number of fitting parameters not exceed the degrees of freedom afforded by the experimental data (which favors fewer strips). Over the years, strip models have been extensively applied in the analysis of X-ray data (Gulik-Krzywicki et al. 1967; Worthington 1969, 1981; Worthington and Blaurock 1969; Wilkins et al. 1971; Franks et al. 1982; McDaniel and McIntosh 1986; McIntosh and Holloway 1987; Wiener et al. 1989; Riske et al. 2001) and neutron data (White and King 1985; King and White 1986; Mason et al. 1999; Pencer and Hallett 2000; Balgavý et al. 2001; Pencer et al. 2005; Qian and Heller 2011). Thorough discussions of strip models and their variants can be found in (Kučerka et al. 2004; Kiselev et al. 2006; Pencer et al. 2006).

For protiated lipid in H_2O, X-ray and neutron SLD profiles are superficially similar in appearance despite the fact that the two techniques are sensitive to different parts of the bilayer (compare Fig. 2a, b). The NSLD profile has been modeled with four strips, which from the bilayer center outward correspond to the methyl trough, methylene plateau, headgroup and water layer (King and White 1986). In an analysis of X-ray data for gel phase DPPC bilayers, Wiener et al. found that a fifth strip, located in the headgroup region, was required to achieve good agreement between structural parameters derived from the strip model and a more complicated hybrid Gaussian/strip model (Wiener et al. 1989). However, for a protiated lipid bilayer in D_2O, the form of the NSLD profile is markedly different compared to a lipid bilayer in H_2O, as the large positive scattering length of deuterium raises the edges of the profile relative to the hydrogen-rich bilayer core (Fig. 2c). The contrast between the methyl trough and the methylene plateau is substantially de-emphasized, which allows for the elimination of one strip by combining the two regions into a single strip representing the hydrocarbon core (Kučerka et al. 2004).

Gaussian and hybrid models

A frequent criticism of strip models is the sharp discontinuity at strip boundaries, which leads to artifactual oscillations in the high q region of $F(q)$ (Wilkins et al. 1971; Wiener et al. 1989; Liu and Nagle 2004). More recently, variations of the strip model have been introduced that join the inner and outer strips with linear functions in an attempt to more closely mimic the smooth profiles obtained from direct Fourier synthesis (Kučerka et al. 2004; Kiselev et al. 2006; Pencer et al. 2006; Kučerka et al. 2007a). However, an alternative to strip models is to represent SLD features with Gaussians, and many examples of this approach can be found for X-ray (Rand and Luzzati 1968; Lemmich et al. 1996; Pabst et al. 2000) and neutron (King and White 1986; Pencer et al. 2006) data. Typically, two Gaussians are used to describe the bilayer, one each for the headgroup and the methyl trough (Fig. 2d). In addition to strictly strip or Gaussian models, hybrid models have been proposed that combine features from both. For example, Wiener et al. modified the standard X-ray Gaussian model by adding a hybrid baseline consisting of strips for the water and methylene regions, joined with a smooth bridging function (Wiener et al. 1989). Interestingly, it was concluded that a simple strip model yielded similar structural parameters for gel phase DPPC bilayers, compared to their hybrid model, provided that both models incorporated two structural features in the headgroup region (Wiener et al. 1989). Finally, a classical error function adopted from reflectometry modeling approaches (Schalke et al. 2000) has been utilized in hybrid models to replace strip functions (Klauda et al. 2006) or Gaussians, by combining these error functions in pairs (Shekhar et al. 2011).

Models for multicomponent bilayers

Nearly half of all known proteins interact in some manner with membranes, and the study of these interactions is one of the frontiers of structural biology. Furthermore, the functional membrane raft has in recent years emerged as a paradigm for explaining a variety of membrane-related phenomena and has generated increased interest in the detailed structures of cholesterol-containing bilayers. Complex mixtures of lipids and protein present considerable challenges for structure determination. A fruitful approach has been to establish a baseline structure for a single-component bilayer, which is then perturbed by the addition of a molecule of interest and modeled with an appropriate modification to the SLD profile. Kučerka et al. (2007a) applied this bottom-up approach to examine the effect of cholesterol on a series of monounsaturated PC bilayers using a modified NSLD strip model to account for the incorporation of cholesterol into the bilayer's hydrocarbon core. Using X-ray scattering, Tristram-Nagle and coworkers studied the interactions of several peptides in model membrane systems using a hybrid SLD model that included an additional Gaussian for the peptides (Greenwood et al. 2008; Pan et al. 2009; Tristram-Nagle et al. 2010). Taking one example, it was determined that a CRAC motif peptide from the gp41 protein of HIV-1 inserts just inside the headgroup phosphate in an SOPC bilayer, leading to bilayer thinning (Greenwood et al. 2008). Importantly, the authors found that bilayer structural parameters could not be reliably obtained in the three-component SOPC/cholesterol/peptide mixtures because of over-parameterization. As will be discussed presently, even

single component bilayer structures are under-determined when considering standalone neutron or X-ray data sets. Significant progress has recently been made through the joint refinement of multiple independent data sets, leading to more robust determination of structural parameters for single component systems. Future work will no doubt include a greater emphasis on multicomponent mixtures, where over-parameterization is a significant barrier to progress that can be overcome through joint refinement, provided enough independent data sets are available.

Resolution considerations for fluid bilayers

Strip and Gaussian models are often able to adequately reproduce scattering data with a minimal number of parameters—an important consideration when dealing with standalone X-ray or neutron data sets. This raises the question: How many scattering features are in principle resolvable from bilayer scattering data? Wiener and White demonstrated that the thermal disorder of a bilayer (disorder of the first kind) is an intrinsic limitation on the number of resolvable structural features from a diffraction experiment of liquid crystalline bilayers. The canonical bilayer resolution is defined as the lamellar repeat distance, d, divided by the maximum number of observable diffraction orders $h_{\max}$ (Wiener et al. 1991). A fully resolved bilayer model will consist of features with widths approximately equal to the canonical resolution, from which it is then trivial to show that the number of structural pieces p required for a complete description of the bilayer is approximately equal to $h_{\max}$ (Wiener and White 1992a). Equivalently, for a continuous form factor extending to $q_{\max}$, p is approximately equal to $d{\cdot}q_{\max}/2\pi$. By this criterion, a fully resolved fluid phase bilayer is typically described by 5–8 features requiring the specification of 10–24 parameters, depending on the type of model used. From this argument, it is clear that a major disadvantage of standalone data is the limited degrees of freedom—neutron or X-ray scattering data sets in isolation do not contain enough information to provide a fully resolved structure, especially in the case of fluid phase bilayers, which are intrinsically of lower resolution. What therefore emerges from a standalone model is a less detailed picture of the bilayer, in which the compositions of the structural groups specified by the model are not well-defined, and which may not adequately describe the molecular organization of the bilayer. Consequently, fundamental bilayer thicknesses (i.e., the total bilayer thickness D_B, and the hydrocarbon thickness $2D_C$) do not necessarily coincide with strip boundaries, or are not related in a simple way to the positions and widths of the Gaussian features, with the unfortunate consequence that lipid area A may not be robustly determined from a standalone analysis.

A distinct advantage of the use of models is the incorporation of additional information, for example, volumetric data determined independently from experiment or simulation (Petrache et al. 1997). Furthermore, the information from X-ray and neutron scattering data can be combined into a joint refinement procedure. By increasing the available degrees of freedom, the bilayer can be modeled at its characteristic resolution—that is, in terms of an appropriate number of molecular components, each of well-defined composition. In a model with clearly defined component groups, the various bilayer thicknesses have natural definitions in terms of Gibbs dividing surfaces, which in turn provide a robust determination of lipid area through equivalent slab relationships between bilayer thickness and independently determined lipid volumes (Nagle and Tristram-Nagle 2000b; Kučerka et al. 2008). For the joint refinement of X-ray and neutron data, it is therefore necessary to take a more systematic approach of modeling the matter distribution of molecular moieties.

Matter density-based models and joint refinement

Matter density-based models are motivated by the fact that bilayer structure is independent of the type of radiation with which it is interrogated—i.e., the individual NSLD and ED profiles are each extensions of the more fundamental matter density distribution. The SLDs are obtained simply by scaling the volume distributions of the chemical moieties with the appropriate scattering lengths. As a result, matter density-based models can easily accommodate different contrast data sets.

A matter density model must first specify the composition of the distinct scattering components making up the bilayer, which is accomplished by parsing the lipid into sub-molecular fragments in a trial and error process. An example of two potential component groupings for the PC headgroup is shown in Fig. 3. A successful parsing divides the lipid molecule into a number of fragments commensurate with the resolution of the data and whose distributions are well described by simple functional forms. Furthermore, the same functional form must apply to both the neutron and X-ray data to within a scaling factor. To address the latter point, Wiener and White projected the atomic coordinates from the crystal structure of dimyristoylphosphatidylcholine (DMPC) onto the bilayer normal, and then calculated the neutron and X-ray centers-of-scattering for various atomic groupings (Wiener and White 1992a). This method gives a rough estimate of the alignment of NSLD and electron density (ED) profiles, though it does not account for the effects of thermal disorder, nor does it test the validity of applying a Gaussian lineshape to the different moiety profiles.

More recently, MD simulations have proven particularly useful for choosing between various parsing schemes. The

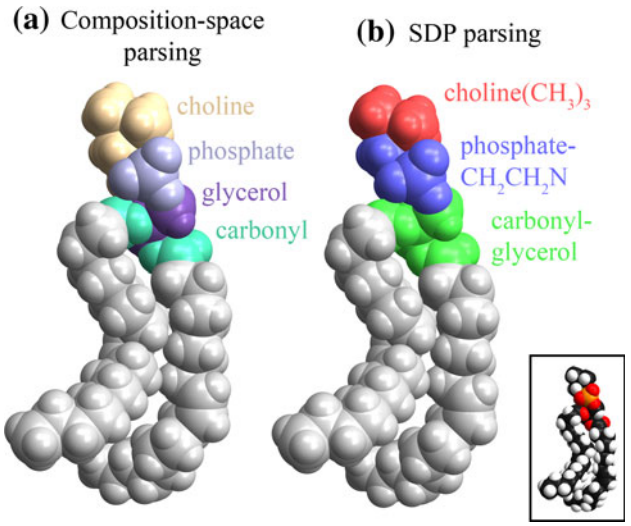

Fig. 3 Two possible component groupings for the phosphatidylcholine (PC) headgroup, demonstrated with a space-filling DOPC model. (**a**) The choline (*gold*), phosphate (*light blue*), glycerol (*purple*) and carbonyl (*cyan*) components used in the composition-space model (Wiener and White 1992b). (**b**) In the scattering density profile (SDP) model (Kučerka et al. 2008), the choline methyls comprise a separate component (*red*). The remaining CH_2CH_2N moiety of the choline is grouped with the phosphate (*blue*), and the carbonyl and glycerol are combined into a single component (*green*). The lipid's hydrocarbon chains are shown in grayscale. *Inset* to the figure shows a space-filling model of DOPC with CPK coloring

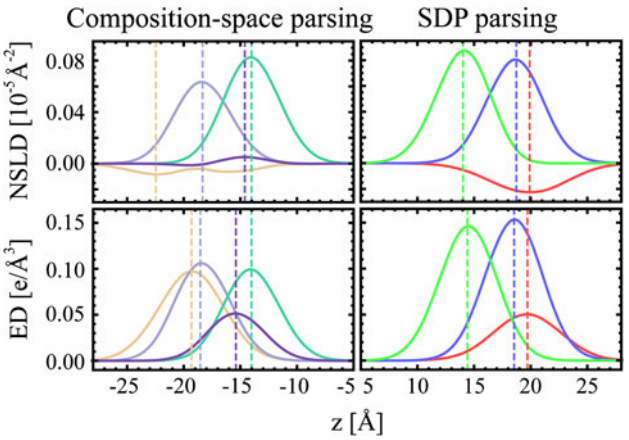

Fig. 4 The composition-space (CS) and SDP parsing schemes for the PC headgroup. Scattering length density (SLD) distributions are calculated individually for each atom in an MD simulation (Kučerka et al. 2008), and summed according to either the CS or SDP atomic groupings (component group coloring as in Fig. 3). NSLD profiles using CS groupings (*upper left*) show non-Gaussian distributions for the choline (*gold*) and glycerol (*purple*) groups. SLD peaks (*dashed lines*) for these groups do not align with corresponding peaks in the electron density distributions (*lower left*). With SDP groupings, NSLD (*upper right*) and ED (*lower right*) component distributions are nearly Gaussian and aligned, such that a single Gaussian volume distribution is sufficient to describe both profiles when scaled by the appropriate scattering length, as described in the text

effects of thermal disorder are inherently accounted for by the simulation, and it is also straightforward to calculate number density distributions for each atom in the simulation. A particular parsing scheme is then easily inspected by summing the atomic neutron (X-ray) scattering distributions according to the proposed atomic groupings. Using this simulation-based approach, Kučerka et al. found that protiated choline has an asymmetric NSLD distribution due to the negative neutron scattering length contribution from the methyl hydrogens, which results in a misalignment of the NSLD and ED peaks, as shown in Fig. 4 (left panels) (Kučerka et al. 2008). However, by grouping the choline methyls into a single fragment, and combining the choline CH_2CH_2N moiety with the phosphate, a headgroup parsing scheme was achieved that maintained the center of scattering gravity for NSLD and ED profiles of the protiated lipid, as well as for deuterated variants of the PC headgroup (Fig. 4, right panels). Inspection of the various parsing schemes is aided by SIMtoEXP, an open access computer program designed to facilitate the comparison of simulation and experimental data (Kučerka et al. 2010).

Composition-space model

After the lipid has been parsed into component groups, an appropriate functional form must be specified for each group of atoms. Individual atoms exhibit approximately Gaussian distributions because of thermal disorder, though substantial overlap of the distributions of adjacent atoms precludes their individual resolution—this is a defining characteristic of fluid phase bilayers (Wiener and White 1992a). Therefore, the most physically realistic functional form for small groups of neighboring atoms is a Gaussian of appropriate width. In a pioneering study, Wiener and White (1992b) proposed a "composition-space" model for a partially dehydrated, fluid phase DOPC bilayer composed of ten Gaussians—four describing the PC headgroup (i.e., carbonyl, glycerol, phosphate and choline, as shown in Fig. 3a), five within the hydrocarbon chain (three for the elongated methylene distribution, and one each for the methine and terminal methyl groups), and one for the water layer. Each Gaussian was described by its position, width and area (which is related to the moiety composition, and therefore fixed by the parsing scheme). The distributions for the double bond, water and terminal methyls were independently determined, leaving 16 free parameters. The DOPC bilayer structure was then solved by jointly refining the neutron and X-ray diffraction data, with each data set contributing eight structure factors (i.e., a marginally determined system where the number of parameters equals the number of observations).

Although volume is globally conserved in Wiener and White's composition-space model, ideal packing within the

unit cell is not intrinsically enforced by the model or the refinement procedure, leading to RMS deviations in local volume of ~7 % in the best-fit structure (Wiener and White 1992b). Using the Weiner et al. data (Wiener and White 1992a), Armen et al. (1998) implemented local volume conservation as a soft constraint (i.e., allowed to vary within some limits) using component volumes obtained from MD simulations. The end result was a better fit to the original data (Armen et al. 1998). Moreover, the additional volume data permitted more parameters to vary in the fitting procedure. By incorporating MD data in the model's refinement process, Armen et al. highlighted the synergistic relationship between simulation and experiment, and pointed the way toward a more robust structural analysis of the bilayer.

The scattering density profile (SDP) model

Solving the structures of biologically relevant, fully hydrated lipid bilayers is a longstanding goal of membrane biophysics (Nagle and Tristram-Nagle 2000a). Scattering data from ULV suspensions have proven important in this endeavor, as ULVs achieve full hydration without the complications of the sample preparation associated with aligned multibilayer stacks and the smearing of Bragg reflections due to increased bilayer undulations (Lyatskaya et al. 2001). However, the use of ULVs comes at the cost of decreased signal-to-noise, and as a consequence, a reduced range of data in q. The addition of volumetric data from MD simulations increases the amount of information that can be used in the model's refinement procedure (Armen et al. 1998; Klauda et al. 2006; Kučerka et al. 2008; Petrache et al. 1997), as does the use of different contrast neutron data sets (e.g., the use of a protiated lipid bilayer at several D_2O/H_2O ratios or deuterated variants of the same lipid) (Kučerka et al. 2008). Importantly, the number of free parameters in the model can be reduced by representing the total hydrocarbon probability as an error function, instead of the sum of three Gaussians (Klauda et al. 2006). Building on these concepts, Kučerka et al. introduced the Scattering Density Profile (SDP) bilayer model, which has since been applied successfully to solving the structure of a variety of PC (Kučerka et al. 2008, 2009, 2011) and PG (Kučerka et al. 2012; Pan et al. 2012) lipids. Figure 5 shows the SDP representation of a fully hydrated DOPC bilayer.

A separate issue with fully hydrated bilayers concerns the functional form of the water distribution, which is more complicated than the approximately Gaussian functional form that adequately describes water in dehydrated bilayers (Armen et al. 1998; Klauda et al. 2006; Wiener and White 1992b). This problem, however, is circumvented in the SDP model by defining the water distribution implicitly through the ideal packing of the unit cell—i.e., water is allowed to fill all voids in the bilayer (Kučerka et al. 2008). Mathematically, the water probability distribution is the complement of the summed probability of the lipid components, such that the volume probabilities at all points along the bilayer normal add up to unity (Fig. 5 lower panel). This approach assumes the absence of free volume within the unit cell and that the volume of a component group does not depend on its location in the bilayer. The validity of the assumption that water fills all voids in the bilayer is supported by volume probability profiles obtained from MD simulations, which typically show only small local deviations from unity, an observation consistent with local volume conservation (Klauda et al. 2006; Kučerka et al. 2008, 2012; Petrache et al. 1997). Although this definition of the water distribution allows for the unphysical outcome of negative water probability, such an outcome is easily avoided in the fitting procedure by imposing a strong penalty term in the objective function.

In the SDP model, bilayer thicknesses are naturally specified in terms of Gibbs dividing surfaces, which are defined by equality of the integrated probabilities to the left and right of the dividing surface (Nagle and Tristram-Nagle 2000b). For example, the Gibbs dividing surfaces for the hydrocarbon and water distributions are equivalent to the hydrocarbon thickness $2D_C$ and the Luzzati thickness D_B, respectively. Each of these thicknesses is readily obtained from SDP parameters, as shown in Fig. 5 (e.g., $2D_C$ is equal to the width of the hydrocarbon error function), and is in turn related to the lipid area A, through experimentally determined lipid volumes—i.e., $A = 2V_L/D_B = (V_L - V_{HL})/D_C$, where V_L and V_{HL} are the total lipid and headgroup volumes, respectively. In the SDP model the latter relationship appears as a normalization factor in the component distributions, such that A is a free parameter determined by the fit.

The robust determination of A in the case of fully hydrated bilayers is a significant achievement of the SDP model, and one that is particularly important for the emerging field of MD simulations. MD holds great promise for revealing the three-dimensional structure of biomembranes, but many outstanding problems remain. Chief among these are the apparent discrepancies between bilayers simulated with different MD packages, such as GROMACS and CHARMM, underscoring the complexity inherent in the development of force fields, ensembles and the treatment of electrostatics. Simulations have a greater claim to validity when they are able to reproduce experimentally observable structural parameters. In particular, A has typically served as the primary validation for bilayer simulations owing to its direct relationship with other bilayer structural and dynamical properties (Anezo et al. 2003; Klauda et al. 2006). Anezo et al. (2003) have noted

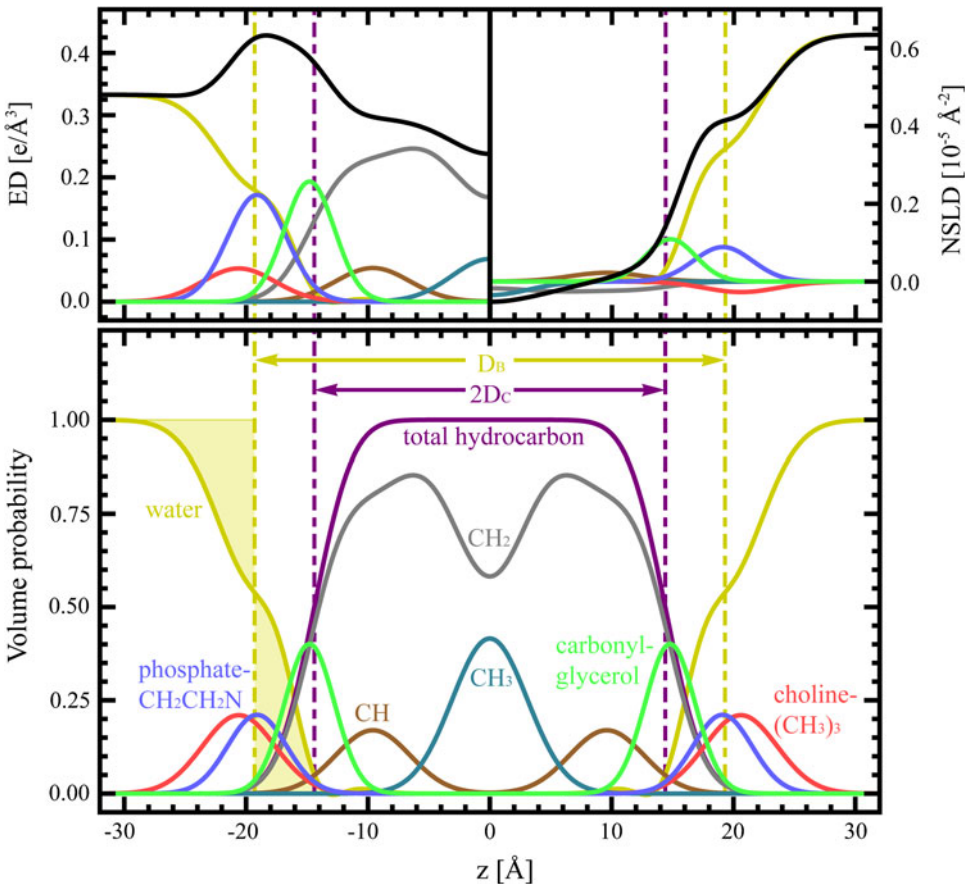

Fig. 5 SDP model representation of a DOPC bilayer (Kučerka et al. 2008). (*Upper*) Electron densities (*left*) and neutron scattering length densities (*right*) of the various component distributions in a lipid bilayer, including the total scattering length density (*solid black lines*). (*Lower*) Volume probability distributions, where the total probability equals 1 at each point across the bilayer (z). The concept of the Gibbs dividing surface is shown for the water distribution, whose mean position is defined by the equality of the *shaded areas*

that regardless of the particular force field or simulation methodology used, simulations that are able to correctly reproduce lipid areas give rise to realistic bilayer properties. For many classes of lipids, the lack of such experimentally determined structural data stands as an impediment to the improvement of force fields and simulation methodologies.

We have recently used the SDP model to obtain structural information, including bilayer thicknesses and A for a number of neutral zwitterionic PC and singly charged anionic PG lipids. In the following section, we provide some highlights from these two classes of lipids from data obtained via SDP analysis.

The application of the SDP model to PC and PG bilayers

Unexpected area per lipid in DOPC bilayers

The first SDP model was developed by Kučerka et al. to look at the detailed structure of fluid phase DPPC and DOPC bilayers (Kučerka et al. 2008). MD simulations used to guide the development of the PC model employed the CHARMM lipid force field version 27 (Klauda et al. 2005). The usual periodic boundary conditions were applied, and the simulation was carried out using 288 lipids (i.e., 144 lipids per leaflet), 32.5 water molecules/lipid, and a temperature of 298 K, with the remaining simulation details given in (Kučerka et al. 2008). The newly developed SDP model was then used to analyze different contrast scattering data collected from DPPC and DOPC bilayers.

DPPC bilayers are the prototypical model membrane system whose various phases have been studied extensively using a multitude of physical techniques (see Nagle and Tristram-Nagle 2000b, and references therein). SDP structural data from DPPC bilayers at 50 °C were found to be consistent with some of the published data, including the much-sought-after area per lipid, which was determined to be 63 Å^2. However, in the case of DOPC bilayers, significant discrepancies were found for the SDP-determined structure compared to values obtained from standalone neutron or X-ray analyses, especially with regard to A.

As previously mentioned, a lipid's lateral area is generally thought to influence lipid-lipid and lipid-protein interactions. Importantly, A plays a central role in the parameterization of MD force fields. In the case of DOPC bilayers, the area of 67.4 Å^2 determined by the SDP model (Kučerka et al. 2008) was nearly 10 % smaller than a previously reported value that was obtained solely through

the analysis of X-ray scattering data (Kučerka et al. 2005; Pan et al. 2008). The main source of this difference is rooted in a constant distance assumption (D_{H1}) found in the standalone X-ray model—i.e., the distance between the electron-dense phosphate group and the Gibbs dividing surface of the hydrocarbon chain region was fixed to a value obtained from an earlier study of gel phase DMPC (Tristram-Nagle et al. 2002). However, as was emphasized by Kučerka et al. (2008), D_{H1} is likely to be specific to individual lipid species and is sensitive to how the MD simulations are performed. Indeed, substantial variation of D_{H1} has been observed based on the SDP model analysis for lipids with different hydrocarbon chain compositions and headgroup moieties (Kučerka et al. 2011; Pan et al. 2012). An overestimation of D_{H1} in the standalone X-ray model will result in a smaller hydrocarbon thickness $2D_C$, and consequently a larger lipid area. On the other hand, such an assumption is not enforced in the jointly refined SDP model. Thus, values of A obtained from the SDP model and aided by more comprehensive experimental data (i.e., different contrast neutron and X-ray scattering data) should be more accurate.

The area per lipid and the position of the double bond in di-monounsaturated PCs

Kučerka et al. (2009) used the SDP model to determine the effects of acyl chain length and double-bond position on the structure of fully hydrated, fluid PC bilayers containing one double bond per acyl chain (diCn:1PC, where $n = 14$, 16, 18, 20, 22 and 24 is the number of acyl chain carbons). For bilayers with $n = 14$ to 18, the double bond was at the 9-*cis* position, whereas for $n = 20$ to 24 bilayers, the double bond was at the 11-*cis*, 13-*cis* and 15-*cis* positions, respectively.

Figure 6 shows that the overall bilayer thickness D_B does not change linearly with increasing acyl chain length, as is the case in commonly studied PC bilayers (Kučerka et al. 2011). More surprisingly, an inverse parabolic dependence of A on the acyl chain length was observed, with a maximum area per lipid near $n = 18$ (i.e., diC18:1PC). The nonlinear behavior of D_B and A can be reconciled in terms of the effects of hydrocarbon chain length and double bond position. Generally speaking, an increase of the hydrocarbon chain length results in increased van der Waals attractive forces, which orders the chains and causes A to decrease (Karlovská et al. 2006). This qualitatively explains the decrease of A when chain length increases from 18 to 24 carbons. On the other hand, the introduction of a double bond disrupts the packing of hydrocarbon chains causing the bilayer to expand laterally (i.e., an increase in A). Such a disordering effect is dependent on the double bond position, with the greatest

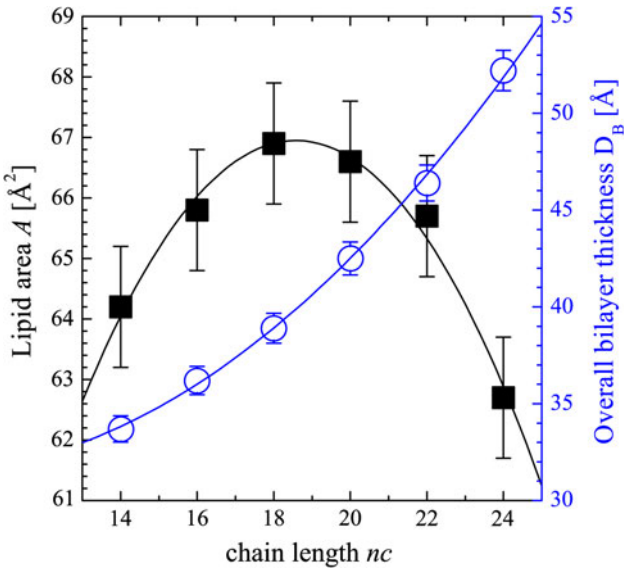

Fig. 6 Bilayer structural parameters for PC lipids obtained through the simultaneous analysis of X-ray and neutron scattering data (Kučerka et al. 2009). Area per lipid (*black squares*) and overall bilayer thickness D_B (*blue circles*) are plotted as a function of chain length, *nc*. Data were fit with a quadratic function (Kučerka et al. 2009)

disorder presumably taking place when the double bond is located in the middle of the hydrocarbon chain (i.e., the double bond's position is fixed relative to the lipid's headgroup, as was the case for the 9-*cis* position lipids). This qualitatively explains the increase of A when chain length increases from 14 to 18 carbons. The experimental results were also found to be in good agreement with MD simulations based on the MARTINI model (Marrink et al. 2007).

Comparison of PC with PG bilayer structures

PG lipids are important anionic components commonly found in bacterial membranes. Reports from MD simulations using the GROMACS force field indicate the area of POPG to be considerably smaller than that of its neutral POPC counterpart at 37 °C (i.e., 55 Å^2 vs. 65 Å^2) (Elmore 2006; Zhao et al. 2007), despite the supposed presence of electrostatic repulsion between PG headgroups (Zhao et al. 2007). This counterintuitive result was attributed to enhanced intra- and inter-molecular hydrogen bonding in PG bilayers. On the other hand, simulations using the CHARMM27 force field reported a POPG area of between 65 and 66 Å^2 (Henin et al. 2009; Tolokh et al. 2009). In light of such contradictory data, the need for an accurate, experimentally determined PG lipid area was clear.

Kučerka et al. (2012) recently formulated an SDP model for PG headgroup lipids guided by MD simulations using the CHARMM27 force field—the reader is reminded that

MD simulations are used only to guide the lipid parsing scheme and have no bearing on the modeling of experimental scattering data for the determination of bilayer structure. In the same study, the model was subsequently used to analyze different contrast neutron and X-ray scattering data for POPG at 30 °C, and an area per lipid of 66 Å^2 was determined. This value is more consistent with that obtained from MD simulations using the CHARMM27 force field, as compared to the GROMACS force field. However, even for the CHARMM27 force field, a non-zero surface potential was required in order to obtain the same area per lipid as the experimentally determined value (Kučerka et al. 2012), indicating the necessity of further refinements to the existing force field.

Using the same SDP model for PG headgroups, Pan et al. investigated the bilayer structures of several commonly used PG lipids in the biologically relevant fluid phase (Pan et al. 2012). An illustrative example from this study is shown in Fig. 7, and a number of conclusions can be drawn from the data. First, lipid area decreases with increasing chain length, regardless of the headgroup moiety. This observation is consistent with the overriding role played by chain-chain attractive interactions. Second, the difference between PG and PC areas is small at infinite chain length (i.e., $1/nc = 0$), implying that these two classes of lipids have a similar steric limit. Since the limiting area of two gel phase chains (for which the chain steric limit is reached) is much smaller than 60 Å^2 (Sun et al. 1996), this observed limiting area is most likely the result of steric interactions between neighboring headgroups. A common feature shared by PG and PC headgroup lipids, and which affects lateral packing, is the glycerol backbone moiety residing at the polar/non-polar interface. This notion is particularly intriguing when one considers the broad spectrum of membrane properties affected by the glycerol backbone, especially when it is chemically altered (Brezesinski et al. 1995; Guler et al. 2009). Third, as hydrocarbon chain length decreases from infinity, interactions other than headgroup steric constraints become increasingly important. The additional repulsive electrostatic interactions between anionic PG headgroups most likely contribute to the larger areas of these lipids (Pan et al. 2012). The aforementioned mechanism qualitatively explains the greater difference in A between PG and PC lipids at shorter chain lengths, with the largest difference observed at zero chain length (Fig. 7b). Although $nc = 0$ does not correspond to a realistic condition, this limiting area per lipid reflects solely the headgroup's contribution to A, without the influence of the hydrocarbon chains.

Lipid areas play a central role in regulating membrane permeability and stability. The newly obtained areas for charged lipids are consistent with the finding that the introduction of anionic lipids into bilayers reduces membrane rupture pressure (Shoemaker and Vanderlick 2002). Moreover, the larger areas associated with the charged PG lipids may facilitate biological processes, including protein translocation (Devrije et al. 1988), bacterial membrane permeability (Nikaido and Vaara 1985) and membrane protein folding (Seddon et al. 2008).

Conclusions

In reconstructing the bilayer scattering length density profile, model-based techniques offer several advantages over direct Fourier reconstruction. Importantly, they allow for the combined use of different types of complementary

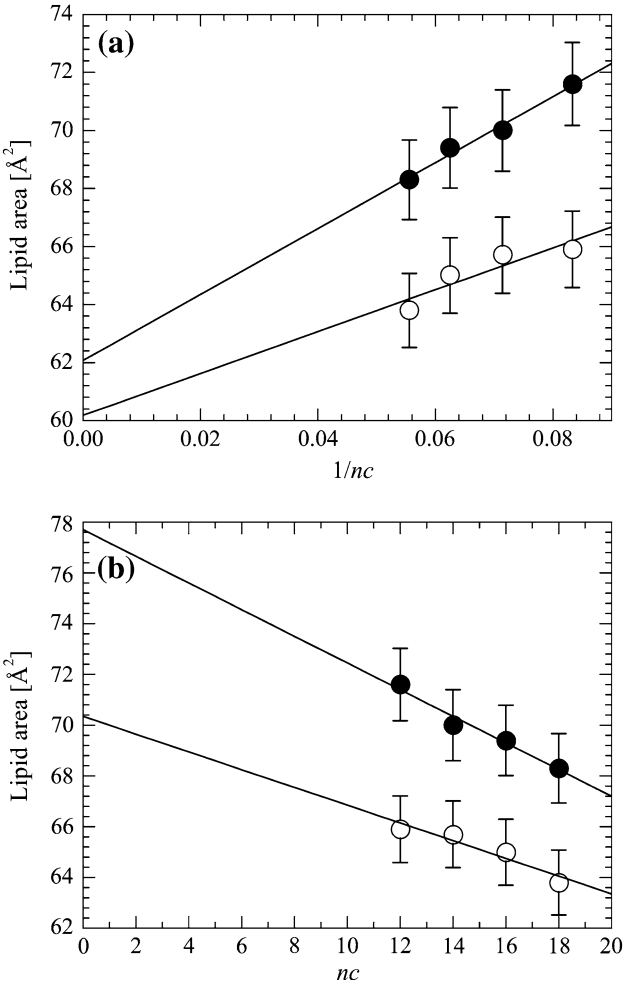

Fig. 7 Areas of saturated PC and PG lipids at 60 °C as a function of chain length, nc. (**a**) Extrapolation of lipid area A to infinite chain length (i.e., $1/nc = 0$) reveals a similar steric limit for PC (*open circles*) and PG (*filled circles*) lipids. (**b**) Extrapolation to zero chain length reveals the contribution of electrostatic repulsion to the increased area of negatively charged PG, compared to neutral PC lipids

data in the analysis, resulting in robust models. We have developed an SDP model that allows for the detailed structure of fluid phase, fully hydrated bilayers through the joint refinement of different contrast neutron and X-ray data sets. A key achievement of the SDP model is its robust determination of lipid areas and bilayer thicknesses.

To date, the application of the SDP model to two major classes of biological lipids (PC and PG) has revealed a number of unexpected structural features. One finding is a substantially smaller area for DOPC compared to previously published values obtained using standalone methods, reinforcing the necessity of using different contrast data to accurately determine lipid bilayer structure. With unsaturated lipids, a unique feature was unveiled in terms of the location of the double bond and its effect on bilayer structure. It was found that the maximal area per lipid was achieved for the diC18:1PC lipid with its double bond located at the middle of the hydrocarbon chain, in good agreement with MD simulations. A systematic comparison between singly charged anionic PG and neutral zwitterionic PC lipids indicated that PGs exhibit larger areas per lipid compared to their counterpart PC bilayers, a result that is likely due to repulsive electrostatic interactions between the charged headgroups. The PG lipid areas also indicate that, compared to the GROMACS force field, the CHARMM27 force field can, in some instances, provide a more accurate description of the molecular interactions taking place within the PG lipid bilayer ensemble.

The joint refinement of neutron and X-ray scattering data with the SDP model considerably reduces the uncertainty in the determination of lipid areas and bilayer thicknesses, in comparison to values determined by standalone scattering methods. In general, close agreement is now obtained between lipid areas evaluated using the SDP model and those determined by NMR methods. However, there are still some noteworthy differences, in particular the temperature sensitivity of the structural parameters obtained by these methods (Kučerka et al. 2011; Petrache et al. 2000), that need to be investigated. Applying the SDP analysis to the structures of the remaining major classes of biological lipids (e.g., phosphatidylethanolamine, phosphatidylserine, phosphatidic acid and sphingomyelin) will provide important insights into the functional significance of the lipid diversity found in nature.

Future efforts will focus on extending the SDP method to more complex systems containing mixtures of lipids, in particular those leading to the formation of phase-separated domains (so-called "membrane rafts") and those with integral membrane proteins. These systems present considerable challenges for structure determination. In addition to the continued enhancement of the SDP model, several other developments will be required. One critical need is the further improvement of molecular mechanics force fields for lipids so that simulations can correctly reproduce and ultimately predict bilayer structural properties. Moreover, novel, isotopically labeled lipids are needed to generate the data required for the continued development of model parameters and the parsing of lipid structures. These developments, together with inclusion of temporal data, particularly from NMR, neutron spin echo (NSE) and quasi-elastic neutron scattering (QENS), will play a key role in making the transition from static structures (form) to dynamic structures (function) that is central to understanding the rich biology of cellular membranes.

Acknowledgments This work acknowledges the support of the office of Biological and Environmental Research (BER) at Oak Ridge National Laboratory's (ORNL) Center for Structural Molecular Biology (CSMB) through the utilization of facilities supported by the US Department of Energy, managed by UT-Battelle, LLC under contract no. DE-AC05-00OR2275. Facilities located at the National Institute of Standards and Technology (NIST) are supported in part by the National Science Foundation under agreement no. DMR-0944772. Facilities located at the Cornell High Energy Synchrotron Source (CHESS) are supported by the National Science Foundation and the National Institutes of Health/National Institute of General Medical Sciences under National Science Foundation award DMR-0225180. JK is supported by ORNL's Program Development (PD) and Laboratory Directed Research and Development (LDRD) programs. RFS is supported by ORNL's LDRD program.

References

Anezo C, de Vries AH, Holtje HD, Tieleman DP, Marrink SJ (2003) Methodological issues in lipid bilayer simulations. J Phys Chem B 107:9424–9433

Armen RS, Uitto OD, Feller SE (1998) Phospholipid component volumes: determination and application to bilayer structure calculations. Biophys J 75:734–744

Balgavý P, Dubničková M, Kučerka N, Kiselev MA, Yaradaikin SP, Uhríková D (2001) Bilayer thickness and lipid interface area in unilamellar extruded 1,2-diacylphosphatidylcholine liposomes: a small-angle neutron scattering study. Biochim Biophys Acta 1512:40–52

Bangham AD, Standish MM, Watkins JC (1965) Diffusion of univalent ions across the lamellae of swollen phospholipids. J Mol Biol 13:238–252

Brezesinski G, Dietrich A, Struth B, Bohm C, Bouwman WG, Kjaer K, Mohwald H (1995) Influence of ether linkages on the structure of double-chain phospholipid monolayers. Chem Phys Lipids 76:145–157

Büldt G, Gally HU, Seelig A, Seelig J, Zaccai G (1978) Neutron diffraction studies on selectively deuterated phospholipid bilayers. Nature 271:182–184

Büldt G, Gally HU, Seelig J, Zaccai G (1979) Neutron diffraction studies on phosphatidylcholine model membranes. I. Head group conformation. J Mol Biol 134:673–691

Devrije T, Deswart RL, Dowhan W, Tommassen J, Dekruijff B (1988) Phosphatidylglycerol is involved in protein translocation across *Escherichia-coli* inner membranes. Nature 334:173–175

Elmore DE (2006) Molecular dynamics simulation of a phosphatidylglycerol membrane. FEBS Lett 580:144–148

Franks NP, Melchior V, Kirshner DA, Caspar DL (1982) Structure of myelin lipid bilayers. Changes during maturation. J Mol Biol 155:133–153

Greenwood AI, Pan J, Mills TT, Nagle JF, Epand RM, Tristram-Nagle S (2008) CRAC motif peptide of the HIV-1 gp41 protein thins SOPC membranes and interacts with cholesterol. Biochem Biophys Acta 1778:1120–1130

Guler SD, Ghosh DD, Pan JJ, Mathai JC, Zeidel ML, Nagle JF, Tristram-Nagle S (2009) Effects of ether vs. ester linkage on lipid bilayer structure and water permeability. Chem Phys Lipids 160:33–44

Gulik-Krzywicki T, Rivas E, Luzzati V (1967) Structure and polymorphism of lipids: X-ray diffraction study of the system formed from beef heart mitochondria lipids and water. J Mol Biol 27:303–322

Hannun YA, Obeid LM (2008) Principles of bioactive lipid signalling: lessons from sphingolipids. Nat Rev Mol Cell Bio 9:139–150

Hazel JR (1995) Thermal adaptation in biological-membranes—is homeoviscous adaptation the explanation? Annu Rev Physiol 57:19–42

Henin J, Shinoda W, Klein ML (2009) Models for phosphatidylglycerol lipids put to a structural test. J Phys Chem B 113:6958–6963

Hope MJ, Bally MB, Mayer LD, Janoff AS, Cullis PR (1986) Generation of multilamellar and unilamellar phospholipid vesicles. Chem Phys Lipids 40:89–107

Hristova K, White SH (1998) Determination of the hydrocarbon core structure of fluid dioleoylphosphocholine (DOPC) bilayers by x-ray diffraction using specific bromination of the double-bonds: effect of hydration. Biophys J 74:2419–2433

Huang C (1969) Studies on phosphatidylcholine vesicles. Formation and physical characteristics. Biochemistry 8:344–352

Karlovská J, Uhríková D, Kučerka N, Teixeira J, Devínsky F, Lacko I, Balgavý P (2006) Influence of N-dodecyl-N,N-dimethylamine N-oxide on the activity of sarcoplasmic reticulum Ca2+-transporting ATPase reconstituted into diacylphosphatidylcholine vesicles: effects of bilayer physical parameters. Biophys Chem 119:69–77

Katsaras J (1997) Highly aligned lipid membrane systems in the physiologically relevant "excess water" condition. Biophys J 73:2924–2929

Katsaras J (1998) Adsorbed to a rigid substrate, dimyristoylphosphatidylcholine multibilayers attain full hydration in all mesophases. Biophys J 75:2157–2162

Katsaras J, Stinson RH (1990) High-resolution electron-density profiles reveal influence of fatty-acids on bilayer structure. Biophys J 57:649–655

Katsaras J, Watson MJ (2000) Sample cell capable of 100 % relative humidity suitable for X-ray diffraction of aligned lipid multibilayers. Rev Sci Instrum 71:1737–1739

Katsaras J, Raghunathan VA, Dufourc EJ, Dufourcq J (1995) Evidence for a two-dimensional molecular lattice in subgel phase DPPC bilayers. Biochemistry 34:4684–4688

Katsaras J, Tristram-Nagle S, Liu Y, Headrick RL, Fontes E, Mason PC, Nagle JF (2000) Clarification of the ripple phase of lecithin bilayers using fully hydrated, aligned samples. Phys Rev E 61:5668–5677

King GI, White SH (1986) Determining bilayer hydrocarbon thickness from neutron diffraction measurements using strip-function models. Biophys J 49:1047–1054

Kiselev MA, Lesieur P, Kisselev AM, Lombardo D, Aksenov VL (2002) Model of separated form factors for unilamellar vesicles. Appl Phys A 74:S1654–S1656

Kiselev MA, Zemlyanaya EV, Aswal VK, Neubert RH (2006) What can we learn about the lipid vesicle structure from the small-angle neutron scattering experiment? Eur Biophys J 35:477–493

Klauda JB, Brooks BR, MacKerell AD, Venable RM, Pastor RW (2005) An ab initio study on the torsional surface of alkanes and its effect on molecular simulations of alkanes and a DPPC bilayer. J Phys Chem B 109:5300–5311

Klauda JB, Kučerka N, Brooks BR, Pastor RW, Nagle JF (2006) Simulation-based methods for interpreting X-ray data from lipid bilayers. Biophys J 90:2796–2807

Kučerka N, Nagle JF, Feller SE, Balgavy P (2004) Models to analyze small-angle neutron scattering from unilamellar lipid vesicles. Phys Rev E 69:051903

Kučerka N, Tristram-Nagle S, Nagle JF (2005) Structure of fully hydrated fluid phase lipid bilayers with monounsaturated chains. J Membr Biol 208:193–202

Kučerka N, Pencer J, Nieh MP, Katsaras J (2007a) Influence of cholesterol on the bilayer properties of monounsaturated phosphatidylcholine unilamellar vesicles. Eur Phys J E Soft Matter 23:247–254

Kučerka N, Pencer J, Sachs JN, Nagle JF, Katsaras J (2007b) Curvature effect on the structure of phospholipid bilayers. Langmuir 23:1292–1299

Kučerka N, Nagle JF, Sachs JN, Feller SE, Pencer J, Jackson A, Katsaras J (2008) Lipid bilayer structure determined by the simultaneous analysis of neutron and X-ray scattering data. Biophys J 95:2356–2367

Kučerka N, Gallova J, Uhrikova D, Balgavy P, Bulacu M, Marrink SJ, Katsaras J (2009) Areas of monounsaturated diacylphosphatidylcholines. Biophys J 97:1926–1932

Kučerka N, Katsaras J, Nagle JF (2010) Comparing membrane simulations to scattering experiments: introducing the SIMtoEXP software. J Membr Biol 235:43–50

Kučerka N, Nieh MP, Katsaras J (2011) Fluid phase lipid areas and bilayer thicknesses of commonly used phosphatidylcholines as a function of temperature. Biochim Biophys Acta 1808:2761–2771

Kučerka N, Holland BW, Gray CG, Tomberli B, Katsaras J (2012) Scattering density profile model of POPG bilayers as determined by molecular dynamics simulations and small-angle neutron and X-ray scattering experiments. J Phys Chem B 116:232–239

Leftin A, Brown MF (2011) An NMR database for simulations of membrane dynamics. Biochim Biophys Acta 1808:818–839

Lemmich J, Mortensen K, Ipsen JH, Honger T, Bauer R, Mouritsen OG (1996) Small-angle neutron scattering from multilamellar lipid bilayers: theory, model, and experiment. Phys Rev E 53:5169–5180

Levine YK, Wilkins MH (1971) Structure of oriented lipid bilayers. Nat New Biol 230:69–72

Lingwood D, Simons K (2010) Lipid rafts as a membrane-organizing principle. Science 327:46–50

Liu YF, Nagle JF (2004) Diffuse scattering provides material parameters and electron density profiles of biomembranes. Phys Rev E 69:040901(R)

Lyatskaya Y, Liu Y, Tristram-Nagle S, Katsaras J, Nagle JF (2001) Method for obtaining structure and interactions from oriented lipid bilayers. Phys Rev E 63:011907

Marrink SJ, Risselada HJ, Yefimov S, Tieleman DP, de Vries AH (2007) The MARTINI force field: coarse grained model for biomolecular simulations. J Phys Chem B 111:7812–7824

Mason PC, Gaulin BD, Epand RM, Wignall GD, Lin JS (1999) Small angle neutron scattering and calorimetric studies of large unilamellar vesicles of the phospholipid dipalmitoylphosphatidylcholine. Phys Rev E 59:3361–3367

McDaniel RV, McIntosh TJ (1986) X-ray diffraction studies of the cholera toxin receptor, GM1. Biophys J 49:94–96

McIntosh TJ, Holloway PW (1987) Determination of the depth of bromine atoms in bilayers formed from bromolipid probes. Biochemistry 26:1783–1788

Nagle JF, Tristram-Nagle S (2000a) Lipid bilayer structure. Curr Opin Struct Biol 10:474–480

Nagle JF, Tristram-Nagle S (2000b) Structure of lipid bilayers. Biochim Biophys Acta Rev Biomembr 1469:159–195
Nikaido H, Vaara M (1985) Molecular-basis of bacterial outer-membrane permeability. Microbiol Rev 49:1–32
Obrien FEM (1948) The control of humidity by saturated salt solutions. J Sci Instrum Phys Ind 25:73–76
Pabst G, Rappolt M, Amenitsch H, Laggner P (2000) Structural information from multilamellar liposomes at full hydration: full q-range fitting with high quality x-ray data. Phys Rev E 62:4000–4009
Pan J, Tristram-Nagle S, Kučerka N, Nagle JF (2008) Temperature dependence of structure, bending rigidity, and bilayer interactions of dioleoylphosphatidylcholine bilayers. Biophys J 94:117–124
Pan J, Tieleman DP, Nagle JF, Kučerka N, Tristram-Nagle S (2009) Alamethicin in lipid bilayers: combined use of X-ray scattering and MD simulations. Biochem Biophys Acta 1788:1387–1397
Pan J, Heberle FA, Kučerka N, Tristram-Nagle S, Szymanski M, Koepfinger M, Katsaras J (2012) Molecular structure of phosphatidylglycerol bilayers: fluid phase lipid areas and bilayer thicknesses as a function of temperature. Biophys J 102:504a
Pencer J, Hallett FR (2000) Small-angle neutron scattering from large unilamellar vesicles: an improved method for membrane thickness determination. Phys Rev E 61:3003–3008
Pencer J, Nieh MP, Harroun TA, Krueger S, Adams C, Katsaras J (2005) Bilayer thickness and thermal response of dimyristoylphosphatidylcholine unilamellar vesicles containing cholesterol, ergosterol and lanosterol: a small-angle neutron scattering study. Biochim Biophys Acta 1720:84–91
Pencer J, Krueger S, Adams CP, Katsaras J (2006) Method of separated form factors for polydisperse vesicles. J Appl Crystallogr 39:293–303
Petrache HI, Feller SE, Nagle JF (1997) Determination of component volumes of lipid bilayers from simulations. Biophys J 72:2237–2242
Petrache HI, Dodd SW, Brown MF (2000) Area per lipid and acyl length distributions in fluid phosphatidylcholines determined by (2)H NMR spectroscopy. Biophys J 79:3172–3192
Qian S, Heller WT (2011) Peptide-induced asymmetric distribution of charged lipids in a vesicle bilayer revealed by small-angle neutron scattering. J Phys Chem B 115:9831–9837
Raghunathan VA, Katsaras J (1995) Structure of the Lc′ phase in a hydrated lipid multilamellar system. Phys Rev Lett 74:4456–4459
Rand RP, Luzzati V (1968) X-ray diffraction study in water of lipids extracted from human erythrocytes: the position of cholesterol in the lipid lamellae. Biophys J 8:125–137
Rand RP, Parsegian VA (1989) Hydration forces between phospholipid-bilayers. Biochim Biophys Acta 988:351–376
Riske KA, Amaral LQ, Lamy-Freund MT (2001) Thermal transitions of DMPG bilayers in aqueous solution: SAXS structural studies. Biochim Biophys Acta 1511:297–308
Schalke M, Kruger P, Weygand M, Losche M (2000) Submolecular organization of DMPA in surface monolayers: beyond the two-layer model. Biochim Biophys Acta 1464:113–126
Seddon AM, Lorch M, Ces O, Templer RH, Macrae F, Booth PJ (2008) Phosphatidylglycerol lipids enhance folding of an alpha helical membrane protein. J Mol Biol 380:548–556
Shekhar P, Nanda H, Losche M, Heinrich F (2011) Continuous distribution model for the investigation of complex molecular architectures near interfaces with scattering techniques. J Appl Phys 110:102216–10221612
Shoemaker SD, Vanderlick TK (2002) Intramembrane electrostatic interactions destabilize lipid vesicles. Biophys J 83:2007–2014
Singer SJ, Nicolson GL (1972) Fluid mosaic model of the structure of cell-membranes. Science 175:720–731
Spector AA, Yorek MA (1985) Membrane lipid composition and cellular function. J Lipid Res 26:1015–1035
Sun WJ, Tristram-Nagle S, Suter RM, Nagle JF (1996) Structure of gel phase saturated lecithin bilayers: temperature and chain length dependence. Biophys J 71:885–891
Tenchov BG, Yanev TK, Tihova MG, Koynova RD (1985) A probability concept about size distributions of sonicated lipid vesicles. Biochim Biophys Acta 816:122–130
Tolokh IS, Vivcharuk V, Tomberli B, Gray CG (2009) Binding free energy and counterion release for adsorption of the antimicrobial peptide lactoferricin B on a POPG membrane. Phys Rev E 80:031911
Tristram-Nagle SA (2007) Preparation of oriented, fully hydrated lipid samples for structure determination using X-ray scattering. Methods Mol Biol 400:63–75
Tristram-Nagle S, Nagle JF (2004) Lipid bilayers: thermodynamics, structure, fluctuations, and interactions. Chem Phys Lipids 127:3–14
Tristram-Nagle S, Liu YF, Legleiter J, Nagle JF (2002) Structure of gel phase DMPC determined by X-ray diffraction. Biophys J 83:3324–3335
Tristram-Nagle S, Chan R, Kooijman E, Uppamoochikkal P, Qiang W, Weliky DP, Nagle JF (2010) HIV fusion peptide penetrates, disorders, and softens T-cell membrane mimics. J Mol Biol 402:139–153
van Meer G, de Kroon AI (2011) Lipid map of the mammalian cell. J Cell Sci 124:5–8
White SH, King GI (1985) Molecular packing and area compressibility of lipid bilayers. Proc Natl Acad Sci USA 82:6532–6536
Wiener MC, White SH (1992a) Structure of a fluid dioleoylphosphatidylcholine bilayer determined by joint refinement of X-ray and neutron diffraction data. II. Distribution and packing of terminal methyl groups. Biophys J 61:428–433
Wiener MC, White SH (1992b) Structure of a fluid dioleoylphosphatidylcholine bilayer determined by joint refinement of x-ray and neutron diffraction data. III. Complete structure. Biophys J 61:434–447
Wiener MC, Suter RM, Nagle JF (1989) Structure of the fully hydrated gel phase of dipalmitoylphosphatidylcholine. Biophys J 55:315–325
Wiener MC, King GI, White SH (1991) Structure of a fluid dioleoylphosphatidylcholine bilayer determined by joint refinement of x-ray and neutron diffraction data. I. Scaling of neutron data and the distributions of double bonds and water. Biophys J 60:568–576
Wilkins MHF, Blaurock AE, Engelman DM (1971) Bilayer structure in membranes. Nat New Biol 230:72–76
Worthington CR (1969) The interpretation of low-angle X-ray data from planar and concentric multilayered structures. The use of one-dimensional electron density strip models. Biophys J 9:222–234
Worthington CR (1981) The determination of the 1st-order phase in membrane diffraction using electron-density strip models. J Appl Crystallogr 14:387–391
Worthington CR, Blaurock AE (1969) A structural analysis of nerve myelin. Biophys J 9:970–990
Wymann MP, Schneiter R (2008) Lipid signalling in disease. Nat Rev Mol Cell Bio 9:162–176
Young JF (1967) Humidity control in the laboratory using salt solutions—a review. J Appl Chem 17:241–245
Zaccai G, Büldt G, Seelig A, Seelig J (1979) Neutron diffraction studies on phosphatidylcholine model membranes. II. Chain conformation and segmental disorder. J Mol Biol 134:693–706

Zhang YM, Rock CO (2008) Membrane lipid homeostasis in bacteria. Nat Rev Microbiol 6:222–233

Zhang R, Suter RM, Nagle JF (1994) Theory of the structure factor of lipid bilayers. Phys Rev E 50:5047–5060

Zhao W, Rog T, Gurtovenko AA, Vattulainen I, Karttunen M (2007) Atomic-scale structure and electrostatics of anionic palmitoyloleoylphosphatidylglycerol lipid bilayers with Na+ counterions. Biophys J 92:1114–1124